New K isomers in ^{248}Cf

R. Orlandi,[1,*] H. Makii,[1] K. Nishio,[1] K. Hirose,[1] M. Asai,[1] K. Tsukada,[1] T. K. Sato,[1] Y. Ito,[1] F. Suzaki,[1] Y. Nagame,[1] A. N. Andreyev,[1,2] E. Ideguchi,[3] N. Aoi,[3] T. T. Pham,[3] S. Q. Yan,[4] Y. P. Shen,[4] B. Gao,[5] and G. Li[5]

[1]*Advanced Science Research Center, Japan Atomic Energy Agency, Tokai, Ibaraki 319-1195, Japan*
[2]*School of Physics, Electronics and Technology, University of York, Heslington, York YO10 5DD, United Kingdom*
[3]*Research Center for Nuclear Physics (RCNP), Osaka University, Osaka 567-0047, Japan*
[4]*China Institute of Atomic Energy, Beijing 102413, China*
[5]*Institute of Modern Physics, Chinese Academy of Sciences, Lanzhou, Gansu 73000, China*

(Received 28 April 2022; revised 12 August 2022; accepted 24 October 2022; published 2 December 2022)

The nuclear structure of ^{248}Cf was investigated at the Tokai Tandem Accelerator Laboratory of the Japan Atomic Energy Agency. ^{248}Cf was one of the nuclei produced in the ^{18}O + ^{249}Cf multinucleon transfer reaction. An array of Ge and $LaBr_3$ detectors was used to detect the γ rays emitted. More than ten new γ-ray transitions from ^{248}Cf were observed and, for the first time, lifetimes of excited states in the nanosecond range were measured. For the previously known bandhead of the 2^- octupole vibrational band at 592 keV, a lifetime of 6.7(2) ns was found. Another, new isomeric state, with a lifetime of 16.8(5) ns, decays via a 48-keV $E1$ transition to a much longer-lived state lying at 0.9(3) MeV, for which a lifetime larger than ≈200 ns is estimated. For this latter state, the unobserved decay points to $K \geqslant 5$. Considering available theoretical models, possible spin-parity assignments of new states are discussed.

DOI: 10.1103/PhysRevC.106.064301

I. INTRODUCTION

The magic numbers, the famous landmarks of the nuclear shell model, which correspond to the sequential filling of proton and neutron shells, have been experimentally established up to $Z = 82$ and $N = 126$. The next spherical magic numbers, expected to give rise to a region of long-lived superheavy nuclei, the so-called island of stability (IoS), are among the major quests of nuclear science since their predictions in the 1960s [1–4]. Different theoretical models, however, disagree on the location of the next spherical shell gaps, with $Z = 114$ and $N = 184$ most often indicated by microscopic-macroscopic models [4–6] and $Z = 120, 126$ and $N = 174, 184$ by self-consistent approaches based on energy-density functionals and by relativistic mean-field models [7–9]. Although in recent years new elements up to $Z = 118$ were produced [10,11], their isotopes do not have enough of either neutrons or protons to reach the IoS, the heaviest ones being ^{294}Ts($Z = 117, N = 177$) and ^{294}Og($Z = 118, N = 176$) [12].

Shell effects are also pronounced in deformed nuclei near mass numbers $A = 252$ and $A = 270$. Here discontinuities in nuclear properties such as α-decay Q values [13] and partial fission half-lives [10], observed near $(Z, N) = (100, 152)$ and $(Z, N) = (108, 162)$, were interpreted as manifestations of "deformed" shell gaps, i.e., energy gaps separating nucleon orbits in the deformed single-particle spectrum [14,15]. These deformed gaps bring forth a significant enhancement of stability even though they are only about 10–15% the size of spherical shell gaps (when taking as an example ^{208}Pb). In this region, microscopic-macroscopic approaches reproduce the energies and ordering of single-particle orbitals better than density-functional-based and relativistic mean-field models [15]. Just to focus on the deformed gaps pertaining to this work, while the former approaches predict them at $Z = 100$ and $N = 152$ [16], the latter tend instead to indicate $Z = 96$, 98, or 104 and $N = 150$ [17,18]. Through comparison with experimental data, these differences have been related to the energy of high-j orbitals at sphericity [17,18]. A firm experimental knowledge of the underlying single-particle spectrum near the deformed shell gaps is particularly important to foster reliable extrapolations to the superheavy elements in the IoS. Some of the orbitals lying near the Fermi level in these deformed nuclei are in fact substates, lowered by nuclear deformation, of those orbits that ultimately determine the location and size of the next spherical shell gaps [15,17,19]. Isotopes in the region of deformed shell gaps thus constitute a gateway to the IoS, both experimentally and theoretically. One of the best tools to investigate the underlying orbital structure is γ-ray spectroscopy, which is sensitive both to single-particle and to collective properties.

This work focuses on the γ-ray spectroscopic study of ^{248}Cf($Z = 98$, $N = 150$), which lies two protons and two neutrons below the generally accepted $Z = 100$ and $N = 152$ gaps. Although the largest deformation can be expected to occur in ^{252}Fm with both proton and neutron deformed gaps, ^{248}Cf shows a lower $E(2^+)$, i.e., 41.53(6) keV compared with 42.1(13) keV in ^{252}Fm [20], possibly indicating a more deformed shape [15]. In addition, the δ_{2p} proton gap parameter

*orlandi.riccardo@jaea.go.jp

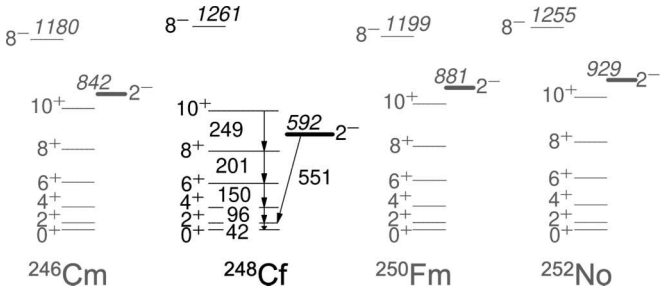

FIG. 1. Partial level schemes of $N = 150$ isotones ^{246}Cm, ^{248}Cf, ^{250}Fm, and ^{252}No. Only the levels of the ground-state rotational band up to the 10^+ state, and the bandheads of the $K^\pi = 2^-$ and $K^\pi = 8^-$ bands, are plotted. In the case of ^{248}Cf, in black, the γ rays currently listed in the ENDSF database [26] are also included and their energies labeled in keV. See text for further details.

[17] shows a maximum at $Z = 100$ for $N = 152$ isotones, but an even larger maximum at $Z = 98$ for $N = 150$ isotones, and no conclusive explanation has been provided for this finding [15]. In the present work, we contribute to the discussion on this region of deformed shell gaps by reporting new γ-ray transitions observed in a recent experiment that extends the currently known level scheme of ^{248}Cf, and by presenting the identification of new isomeric states.

The first experimental information on excited states of ^{248}Cf came from the ^{249}Cf$(d,t)^{248}$Cf reaction, studied with a magnetic spectrograph [21,22]. This neutron pickup reaction populated the ground-state band up to spin 8^+, a $K^\pi = 2^-$ octupole vibrational band at 592 keV up to spin 8^-, and several other excited states lying between 1.2 and 2.7 MeV, belonging to several two-quasiparticle bands built on valence neutron orbitals. The lowest-lying two-quasineutron state, with an assigned $K^\pi = 8^-$ configuration, lies at 1261 keV (see Fig. 1). More than twenty additional small peaks were observed in the triton spectrum, but for these weakly populated states the assignment was either not possible (15 states) or tentative (7 states) [22].

Further experimental information on ^{248}Cf was obtained from the β decay of ^{248}Bk [23], the α decay of ^{252}Fm [24], and from in-beam γ-ray spectroscopy at the JAEA Tandem accelerator [25], which extended the ground-state band up to the 10^+ state. From all these experiments combined, only six γ rays emitted by ^{248}Cf were known [26] (see Fig. 1). The 551-keV $2^- \rightarrow 2^+$ transition (550.7(1) keV in Ref. [23], 550.6(1) keV in this work) was only observed in the β decay of ^{248}Bk [23], where its multipolarity was determined to be $E1$. More recently, via a ^{208}Pb on ^{249}Cf reaction study with Gammasphere at Argonne National Laboratory [27], both the ground-state band and the 2^- octupole band of ^{248}Cf were extended respectively up to spins $26\hbar$ and $25\hbar$. Until now, the lifetime has not been measured for any of the known excited states.

As can be seen in Fig. 1, the $K^\pi = 2^-$ band in ^{248}Cf is the lowest-lying octupole vibrational band among $N = 150$ isotones [15], and also among all Cf isotopes where this band has been observed (^{250}Cf [28], ^{252}Cf [29]). The challenge of reproducing the sudden drop in energy of the 2^- bandhead in ^{248}Cf compared with other $N = 150$ isotones was tackled by a number of theoretical calculations [30–35], with varying degrees of success. Among the different models, the quasiparticle-plus-phonon model [31] and the independent quasiparticle model [36,37], which dates back about 50 years, are those which most closely reproduce the energy of 2^- levels, predicted at 612 keV in ^{248}Cf. According to these models, the main components of the collective 2^--state wave function in ^{248}Cf are the $\nu 9/2^-[734] \otimes \nu 5/2^+[622]$ two-neutron configuration with a weight of 16% and the $\pi 7/2^+[633] \otimes \pi 3/2^-[521]$ two-proton configuration with a weight of 65% [37] or 62% [31]. Other calculations, such as the QRPA calculations by Rezynkina *et al.* [34], predict 66% two-quasineutron and only 34% two-quasiproton component excitations, but exhibit a less pronounced dip in the excitation energy of the 2^- level at $Z = 98$, calculated to lie at 920 instead of 592 keV. We also note that, as an alternative explanation of the sudden energy drop of the 2^- bandhead, it was recently suggested that ^{248}Cf may display a maximum of triaxial octupole (or tetrahedral) deformation (Y_{32}) that alters the single-particle spectrum and generates a shell gap at $Z = 98$ [32].

In this paper, we extend the level scheme of ^{248}Cf, and focus in particular on the isomeric character of three low-lying states. One of these is the 2^- state at 592 keV, shown in Fig. 1, whose isomeric character was unknown prior to this experiment. The other isomers are new low-lying states connected by a 48-keV $E1$ transition. After describing the setup in Sec. II, Sec. III shows the experimental evidence for these new states and their placement in the level scheme. Possible configurations of new isomeric states are discussed in Sec. IV.

II. EXPERIMENTAL DETAILS

The experiment was performed at the Tokai Tandem accelerator facility of the Japan Atomic Energy Agency (JAEA). The 1.2-mm-diameter radioactive target, prepared at JAEA, consisted of 104 μg/cm^2 of ^{249}Cf ($t_{1/2} = 351(2)$ y [38]), electrodeposited on a $\approx$270$-\mu$g/cm$^2-$thick nickel foil. The radioactivity of the ^{249}Cf layer was nearly 300 kBq. The JAEA Tandem accelerator is one of the few facilities in the world where such radioactive actinide targets can be irradiated with beams of heavy ions [39–41]. The ^{249}Cf target was bombarded for about 100 h by a beam of ^{18}O with an energy of 140.4 MeV, approximately 1.3 times the Coulomb barrier. The average beam intensity was $\sim$1 pnA. In the collisions between ^{18}O and ^{249}Cf, several isotopes of Cf, Es, Fm, and No were produced via multinucleon transfer reactions. The nucleus discussed in this work, ^{248}Cf, was produced via the ^{249}Cf$(^{18}$O, ^{19}O$)^{248}$Cf single-neutron pickup reaction (Q value of $-1.631(6)$ MeV [42]). The isotopes were identified on an event-by-event basis by detecting the corresponding light ejectiles using an array of $\Delta E - E$ silicon telescope detectors. The γ rays emitted by the nuclei produced were detected using by an assembly of Ge and $LaBr_3$ detectors. A schematic diagram of the setup is shown in Fig. 2.

The Si array, similar to the one described in Refs. [43,44], was made of ten trapezoidal ΔE detectors of a thickness of either 75 μm (eight detectors) or 50 μm (two detectors),

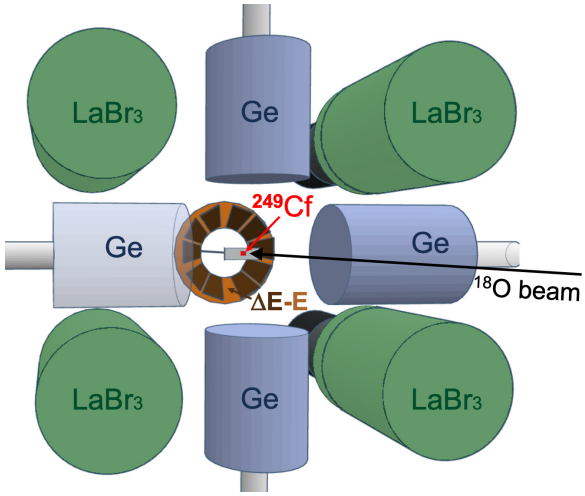

FIG. 2. Schematic diagram of the particle and γ-ray detection setup used in the experiment. Light ejectiles from the reaction are detected in the Si $\Delta E - E$ array, while four Ge and four $LaBr_3$ detectors are mounted in a compact geometry to detect the γ rays from the isotopes produced in the reaction.

arranged in nearly conical geometry in front of a 300-μm-thick single-sided silicon-strip detector (E detector) consisting of two half circles, each comprising 16 concentric strips. This particle detector array, placed 42 mm downstream from the target, covered an angular range from 30.5° to 48.3° in the laboratory frame. Ejectiles from the reaction lose part of their energy (ΔE) when crossing one of the ΔE detectors, and deposit their residual energy ($E_{\rm res}$) when stopping in the E detector, so that $E_{\rm tot} = \Delta E + E_{\rm res}$. Thanks to the highly uniform thickness (<1 μm variation [44–47]) of the ΔE detectors, not only the species (O, N, C, etc.) but also the mass number of each ejectile could be resolved, as can be seen in the ΔE vs $E_{\rm res}$ plot in Fig. 3. The energy calibration of the Si detectors was carried out using the ^{18}O elastic-scattering peak as a reference. The excitation energy ($E_{\rm ex}$) of the corresponding heavy recoil was determined from the measured energy and scattering angle of each identified ejectile, and from the reaction Q value. The underlying assumption is that the light ejectile is in its ground state, which makes the excitation-energy estimate an upper limit. A Gaussian fit to the ^{18}O elastic peak gives a σ of $\approx$0.5 MeV. The uncertainty in the centroid is, however, much smaller since it also depends on the number of counts. For the excited states discussed in this work, the estimated uncertainty in the excitation energy is approximately 200–300 keV.

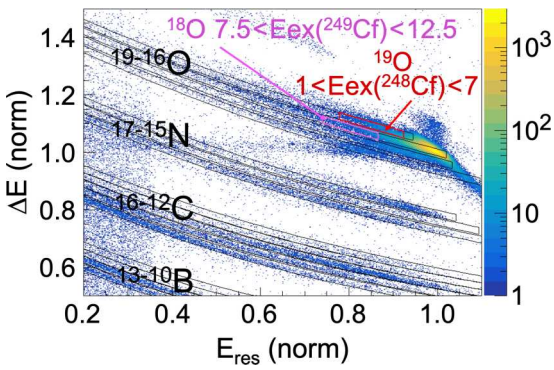

FIG. 3. Typical ΔE vs $E_{\rm res}$ identification plot achieved with the Si array. The data are normalized to the energy of the ^{18}O elastic-scattering peak for each combination of ΔE and E strip. The plot corresponds to one ΔE detector and either of three neighboring strips (5–7) in the E detector, for $\approx$7 h of beam time. Gates on different ejectiles are shown in black. Smaller gates corresponding to narrow excitation energy ranges for ^{248}Cf and ^{249}Cf are also shown.

The γ-ray detector array consisted of four 60%-relative-efficiency coaxial Ge crystals and four large-volume, 4×5 inch ($\phi \times L$) $LaBr_3$ scintillators [48] mounted in a compact geometry as shown in Fig. 2. This detector arrangement resulted in a total absolute photopeak efficiency of 7.6% and 1.6% for the combined Ge detectors at, respectively, 121.8 and 1332.5 keV. At these same energies, for the combined $LaBr_3$ detectors the efficiency was respectively 10% and 5.4%. The average counting rates in each Ge, respectively $LaBr_3$ detector, were approximately 8 kcps (kilocounts per second) and 15 kcps without beam, and about 28 and 38 kcps for a beam intensity of $\approx$1 pnA. For signal processing, analog electronics modules were employed. The energy signals of Ge detectors were amplified using ORTEC and TENNELEC spectroscopy amplifiers with a shaping time of 2 μs. The timing signals of the Ge, as well as the energy and timing signals of the $LaBr_3$ detectors, were processed using Mesytec MSCF-16 shaping/timing filter amplifiers. The difference in energy resolution between Ge and $LaBr_3$ detectors can be appreciated in Fig. 4(b), where the Ge and $LaBr_3$ spectra corresponding to an excitation energy of ^{248}Cf between 1 and 3 MeV are overlaid.

Thanks to their fast timing response, the $LaBr_3$ detectors revealed the presence of isomeric states with lifetimes in the few-nanosecond range. Furthermore, they provide prompt and delayed gates for the coincident Ge detectors. i.e., coincidence windows defined both with respect to the γ-ray peak of interest, and with respect to the timing of the $LaBr_3$ signals (i.e., the time difference between the $LaBr_3$ and the prompt Si-ΔE signals).

The energy and time of detector signals were stored using a triggerless data acquisition system, which recorded the time in timestamps of 50 ns. To search for nanosecond isomers, Time-to-digital (TDC) conversion cards were employed. A TDC channel was reserved for each γ-ray detector. The common START signal for the TDCs was provided by the logic OR signal of the ΔE detectors, while the STOP was given by the delayed logic timing signal of each γ-ray detector. The TDC has a window of nearly 1.6 μs, and a resolution of $\approx$0.2 ns.

III. RESULTS

A. Assignment of transitions to ^{248}Cf

Transitions belonging to ^{248}Cf can be extracted from the collected data in two different ways. In terms of the number of γ-ray peaks observed, the most fruitful way is to gate on ^{19}O, when its detected kinetic energy corresponds to an excitation energy of ^{248}Cf below the neutron separation energy, i.e.,

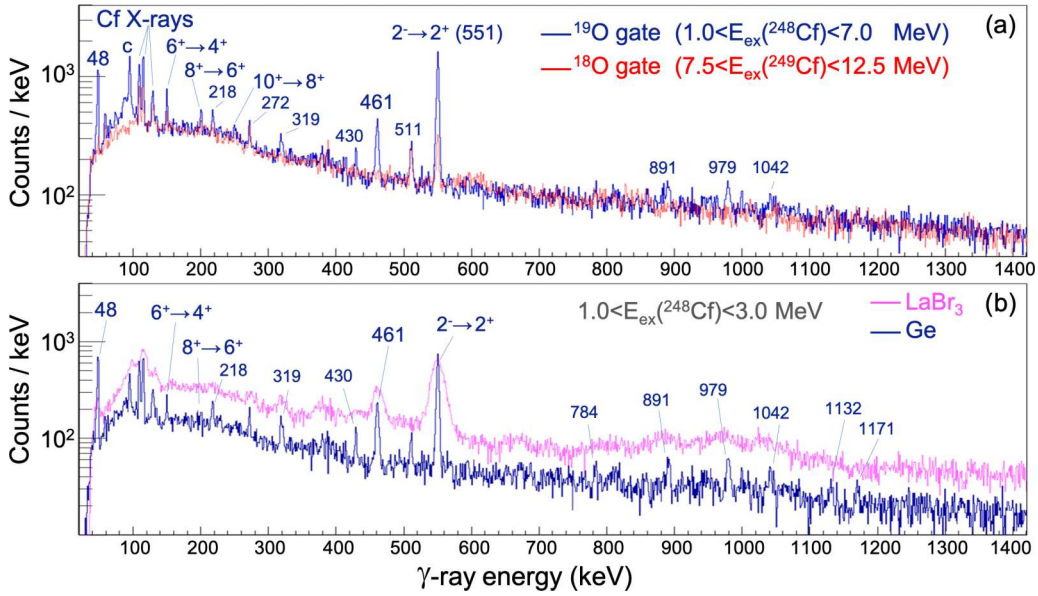

FIG. 4. (a) Ge γ-ray-energy spectra obtained by gating on either ^{19}O for $E_{ex}(^{248}\mathrm{Cf})$ between 1 and 7 MeV (blue line) or ^{18}O for $E_{ex}(^{249}\mathrm{Cf})$ between 7.5 and 12.5 MeV (red line). Previously known ^{248}Cf γ rays are labeled by the spin-parities of the initial $\rightarrow$ final states. Some of the peaks, such as the one at 551 keV, can be seen with either gate. New γ-ray peaks are labeled by the energy in keV, rounded to the nearest integer. The peak labeled "c", at 96 keV, comes from ^{19}O. (b) Ge (blue) and $LaBr_3$ (purple) γ-ray energy spectra gated on ^{19}O for $E_{ex}(^{248}\mathrm{Cf})$ between 1 and 3 MeV.

6.935 MeV [26]. In addition, it is also possible to use as a gate those events of the ^{18}O channel where the excitation energy of ^{249}Cf is above the neutron separation energy, i.e., $E_{ex} > \approx 5.6$ MeV [38], and below the two-neutron separation energy of 12.5 MeV [42]. The gates applied to the data are shown in the particle identification (PID) plot in Fig. 3 (the gate on ^{18}O starts at 7.5 MeV to reduce contaminant γ rays from ^{249}Cf). The γ-ray spectra obtained with these respective gates are shown in Fig. 4(a). While several peaks are clearly visible in both spectra, such as the 551-keV γ ray, some differences also emerge, revealing that some states populated via the (^{18}O, ^{19}O) transfer reactions are not populated by neutron emission from excited ^{249}Cf. The 42-keV $2^+ \rightarrow 0^+$ and 96-keV $4^+ \rightarrow 2^+$ transitions of the ground-state band are not visible due to their very large internal conversion coefficients of, respectively, 1461 and 26.53 [49].

Figure 4(b) shows the overlaid $LaBr_3$ and Ge γ-ray spectra corresponding to a ^{248}Cf excitation energy between 1 and 3 MeV. The relative intensity of different peaks varies depending on the selected excitation-energy range. For example, comparing the ^{19}O-gated Ge spectra shown (in blue) in Figs. 4(a) and 4(b), peaks of the ground-state rotational band can be seen up to spin 10^+ in the E_{ex} range up to 7 MeV, while for an excitation between 1 and 3 MeV [Fig. 4(b)], the $10^+ \rightarrow 8^+$ transition cannot be seen, and the $8^+ \rightarrow 6^+$ γ ray is barely visible. However, in the 1–3-MeV E_{ex} range, new transitions relevant to the current discussion are most strongly populated. Furthermore, it is within this range that several bands were populated in the (d, t) reaction [22], thus this selection permits one to assess whether some of the new transitions may be connecting previously known states.

Figure 5(a) shows the $LaBr_3$ γ-ray energy vs particle-γ-ray time difference, and isomeric transitions can be seen as a tail on the right-hand side of the prompt region, in particular at 551 and 48 keV, as well as a weaker one at 272 keV, which is a contaminant transition from ^{249}Cf [50]. These tails are due to lifetimes of the order of few nanoseconds, and are very difficult to measure with a system consisting only of Ge detectors, which is probably why they were not reported in previous studies.

B. The 48-keV isomeric transition

The 48-keV γ ray [47.8(1) keV in Table I] is among the strongest peaks in the ^{19}O-gated spectrum shown in Fig. 4(b). Together with the 461-keV γ ray [461.1(1) keV in Table I], these transitions are mostly populated in the excitation range between 1 and 3 MeV. The fit of the exponential decay curve of the 48-keV γ-ray, presented in Fig. 5(c), reveals a lifetime of 16.8(5) ns. The fact that such a low-energy transition is so clearly visible suggests a low internal conversion, thus $E1$ multipolarity, as indeed confirmed by the analysis of γ-ray coincidences discussed in the following paragraphs.

Figure 6 shows the Ge spectra obtained by "delayed" and "prompt" $LaBr_3$ gates. Delayed gates correspond to a $LaBr_3$-Si ΔE time difference between 2 and 70 ns, and prompt gates between -2 and 2 ns. Spectra selected by delayed gates for the 551-keV the 48-keV γ rays can be seen respectively in Figs. 6(a) and 6(b). Figure 6(c) results from a prompt gate set on the 461-keV transition. The background spectra, obtained by energy gates set in proximity of the peaks of interest, are plotted for comparison on the the negative y axis. We note that the background spectra are significantly smaller for the 551- and 48-keV gates, thanks to their much higher peak-to-background ratio on the delayed $LaBr_3$ γ-ray spectra. A list of the main coincidences obtained by gates on these peaks

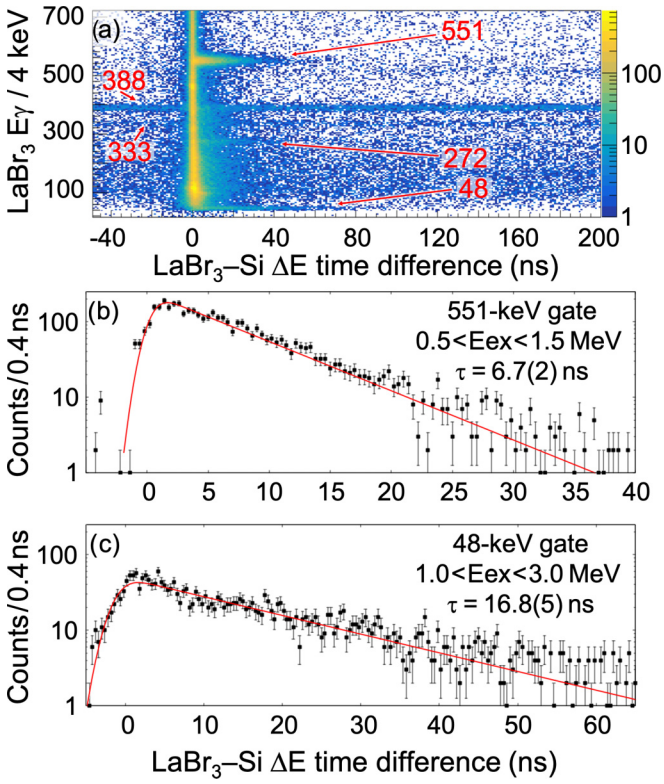

FIG. 5. (a) γ-ray energy vs particle–γ-ray time difference of $LaBr_3$ detectors for events gated on ^{19}O in the particle identification (PID) spectrum, corresponding to the production of ^{248}Cf with $1 < E_{ex} < 3$ MeV. The strongest background γ-ray lines at 333 and 388 keV, from ^{249}Cf radioactivity, are visible on either side of the prompt distribution. Isomeric transitions, which appear only on the right-hand side of the prompt, are labeled in keV. The peak at 272 keV is a γ ray belonging to ^{249}Cf, due to some contamination from the much larger cross section of the ^{18}O channel. (b,c) Lifetime measurements obtained by fitting the distributions resulting from gating the matrix shown in (a) respectively on the 551- and 48-keV γ-ray peaks. The fitted function is the convolution of a Gaussian with an exponential decay.

and on the other ^{248}Cf peaks observed in Fig. 4(b) can be found in Table I. Inspection of Figs. 6(b) and 6(c) clearly implies that the 48-keV isomeric γ ray is coincident with a 461-keV transition. Since, as revealed by Fig. 5(a), the 48-keV transition is isomeric but the 461-keV peak is prompt, the 461-keV γ ray must be the first in the cascade, feeding the state emitting the 48-keV γ ray, either directly or via some mostly converted low-energy transition.

From the analysis of coincidence spectra, the branching of the 48-keV transition was determined. Compared with the feeding 461-keV γ ray, the efficiency-corrected intensity of the 48-keV γ ray is 33(9)%. Such a large fraction clearly points to an $E1$ multipolarity, as the total internal conversion coefficient is 0.999 for an $E1$ transition, 72.66 for $M1$, 724.9 for $E2$, and so forth [49]. Including internal conversion, the 48-keV transition carries 66(18)% of the feeding strength. We notice that this value, within two standard deviations, is also compatible with a branching of 100%. If present, the remaining branching proceeds via other, unobserved transition(s). We also note that the observed 33(9)% branching does not contradict the γ-ray intensities listed in Table I, since the state decaying via the 48-keV transition is also directly populated in the reaction, and possibly fed by additional unobserved γ rays. The $B(E1)$ strength of the 48-keV γ ray is $1.12(30) \times 10^{-4}$ e^2fm^2, or $(4.4 \pm 1.2) \times 10^{-5}$ W.u. (Weisskopf units). The inverse of the transition strength is known as the hindrance factor F_W, which is also equivalent to the ratio of the partial γ-ray lifetime (τ_γ) to the Weisskopf estimate (τ_W), i.e., $F_W = \tau_\gamma / \tau_W$. The hindrance factor roughly scales with the change of the angular momentum projection K on the symmetry axis, ΔK. For the 48-keV transition, $F_W = 2.3(6) \times 10^4$. According to Loebner systematics [51] and the recent review of K-isomer decays [52], this value is consistent with $\Delta K = 0$, 1, or 2.

Neither the 48-keV nor the 461-keV γ rays are in coincidence with the 551-keV γ ray, as shown by all three spectra of Fig. 6. Furthermore, no transition can be found which connects the 48- and 461-keV γ-rays to any other known state. We also extensively examined the energy differences between the levels observed in the (d, t) reaction [22], to identify possible candidates decaying via the 48- and 461-keV transitions, but we could find no group of states, even among those still unassigned, to which these new transitions could be confidently linked.

The main indication concerning the placement of the 48- and 461-keV γ rays in the level scheme comes from γ-ray energy vs $E_{ex}(^{248}\text{Cf})$ matrices such as those presented in Figs. 7(a) and 7(b). Here, the γ-ray energy corresponding to delayed $LaBr_3$ (a) and prompt Ge (b) signals is plotted as a function of ^{248}Cf excitation energy. Projections of these matrices obtained by gating on the 551-, 48-, and 461-keV transitions are shown in Fig. 7(c) and 7(d). The data were fitted using sigmoid functions that model the sudden jump in γ-ray intensity in proximity of the populated excited states. The excitation energy of the states decaying via the 461- and 48-keV γ rays are deduced from the difference with the excitation energy of the known 592-keV state, used as a reference. These matrices and their projections reveal that the level decaying via the 48-keV γ ray lies approximately 0.35 MeV higher in excitation than the 592-keV state, while the one decaying via the 461-keV transition about 0.8 MeV above, i.e., at excitations of about 0.95(30) and 1.4(3) MeV. Consequently, the energy of the state fed by the 48-keV γ ray is estimated to be 0.9(3) MeV.

To confirm our method, we also examined the ^{17}O data which correspond to the production of ^{250}Cf. In this channel, one of the strongest peaks is the 828-keV, $2^- \rightarrow 2^+$ decay of the 871-keV state [28]. In the projection shown in Fig. 7(f), gated by the ^{250}Cf 828-keV γ ray, the first jump in the γ-ray intensity occurs at an excitation energy of 1.03(20) MeV, i.e., in agreement with the expected 871 keV.

In general, in order to include the observed transitions in the level scheme, these principles were followed: (i) the γ-ray-gated excitation-energy spectrum was used to get an indication of the energy of the emitting state, especially when it could not be determined via coincidences alone, as for the 48- and 461-keV transitions; (ii) for new γ rays, all energy

TABLE I. Energy (E_γ) in keV, γ-ray relative intensity (I_γ), emitting state's energy (E_i), and strongest coincidences for the γ-ray peaks which can be seen in the Ge γ-ray spectrum of Fig. 4(b), in the excitation-energy interval $1 < E_{ex}(^{248}Cf) < 3$ MeV. The listed coincidences correspond to peaks appearing in the Ge spectrum selected by gates set on the $LaBr_3$ spectrum. For the 48- and 551-keV peaks, coincidences with the prompt (^{p}) and delayed (^{d}) gates are shown separately. For all other peaks, only those with the prompt gate are shown. The bold font is used for transitions which appear in the level scheme in Fig. 8. For those peaks, tentatively included in the level scheme, which can only be seen in coincidence, I_γ and E_i are provided within square brackets. Superscripts "u" and "k" refer respectively to unplaced or contaminant background peaks. Bracketed γ-ray energies correspond to weak coincident peaks.

E_γ (keV)	I_γ (%)	E_i	Main coincidences
47.8(1)	34(1)	(930)	^{d}**461**,1175^u, (384)^u, 175^u, (323)^u ^{p}588^u
109.6(1)[a]	18(1)		**551**,**48**,637^u, 806^u
115.0(1)[a]	23(1)		**551**,**48**,637^u, 806^u
129.2(2)[b]	9.4(4)		**551**
131.4(3)^u	1.8(5)		
133.7(4)[b]	2.8(5)		**551**
149.7(1)[c]	5.0(7)	287	**201**,1355^u
200.6(1)[c]	2.7(7)	488	109,**150**,173^u, 1465^u
217.7(1)^u	5.9(8)		891^u, 738^u, 660^u, 524^u
319.2(4)^u	5.7(7)		1014^u
429.6(3)	7.3(7)	1022	**551**,833^u, 924^u, 1039^u, 428^u
461.1(1)	31(1)	1391	**48**,582^u, 564^u, 672^u, 96^c
550.6(1)	100(1)	592	^{d}**979**,**1042**,**430**,96^k, (1283)^u,**915**[5(2),E_i:1507], 388^k,**(1176)**[3(1),E_i:2495],(1226)^u, 731^u, 494^u, **727**[2(1),E_i:1319],**(926)**[2(1),E_i:1556],640^u, 599^u, 164^u, 911^u, 323^u, 333^k, 224^u, 271^u, 69^u ^{p}1257^u, 1190^u, 488^u
783.7(4)^u	3.5(7)		
891.1(4)^u	6.5(9)		**551**,1370^u, 218^u
979.4(5)	11.5(9)	(1571)	**551**
1042.0(6)	6.6(9)	(1634)	**551**
1131.6(8)^u	5(1)		
1170.9(6)^u	6(1)		

[a]Cf K_a x rays, unresolved doublet in the $LaBr_3$ spectrum.
[b]Cf K_b x rays, unresolved doublet in the $LaBr_3$ spectrum.
[c]Coincidences for the 1–7 MeV excitation-energy range.

differences between excited states previously known from the (d,t) reaction were considered, taking into account also the uncertainty in the level energies, sometimes as large as 3 keV [22]; (iii) for those cases where spin and parity assignments are available, transitions characterized by a ΔK leading to a long expected lifetime (>100 ns) were excluded. Following these criteria, some of the observed γ rays were in the ^{248}Cf level scheme shown in Fig. 8, albeit tentatively.

C. The 551-keV isomeric transition

The 551-keV 2^-(592 keV) $\rightarrow$ 2^+(42 keV) transition is the strongest peak in the γ-ray spectra of Fig. 4. The fit of the exponential decay curve is shown in Fig. 5(b), for $E_{ex}(^{248}Cf)$ between 0.5 and 1.5 MeV, and reveals a lifetime of 6.7(2) ns. From the known $E1$ multipolarity and $\approx$100% branching ratio [23], a reduced $B(E1)$ transition probability of $5.55(17) \times 10^{-7}$ e^2fm^2 [or $2.18(7) \times 10^{-7}$ W.u.] was deduced.

The delayed character of this transition corresponds to $F_W = 4.59(14) \times 10^6$. This hindrance factor is consistent with $\Delta K = 2$, as indeed expected for this transition [51,52]. This value, however, does not exclude $\Delta K = 1$ or 3, due to the broad distributions of known $E1$ decays vs ΔK shown in Fig. 14 in Ref. [52]. We note that, in the actinide region, the only other measured transition strength from the 2^- octupole vibrational band to the 2^+ state of the ground-state band, in ^{234}U, exhibits an almost identical strength of $1.69(20) \times 10^{-7}$ W.u. [53].

In the coincidence spectrum gated on the delayed component of the 551-keV transition, shown in Fig. 6(a), one of the strongest peaks is found at 430 keV. Considering the energy differences of levels, this coincidence is compatible with a decay from the still unassigned state at 1021(2) keV observed in the (d,t) reaction [22], and was tentatively included in the level scheme of Fig. 8. For other coincidences, i.e., the 979- and 1042-keV peaks, no likely origin could be found among any of the known levels, neither considering the energy difference with the 2^- state, nor with other low-lying states in this vibrational band. From inspection of the excitation-energy spectrum gated on these γ rays, following the same method as shown in Fig. 7, they appear to originate from states approximately 1 MeV above the 592-keV state. We thus tentatively place them in the level scheme assuming that they

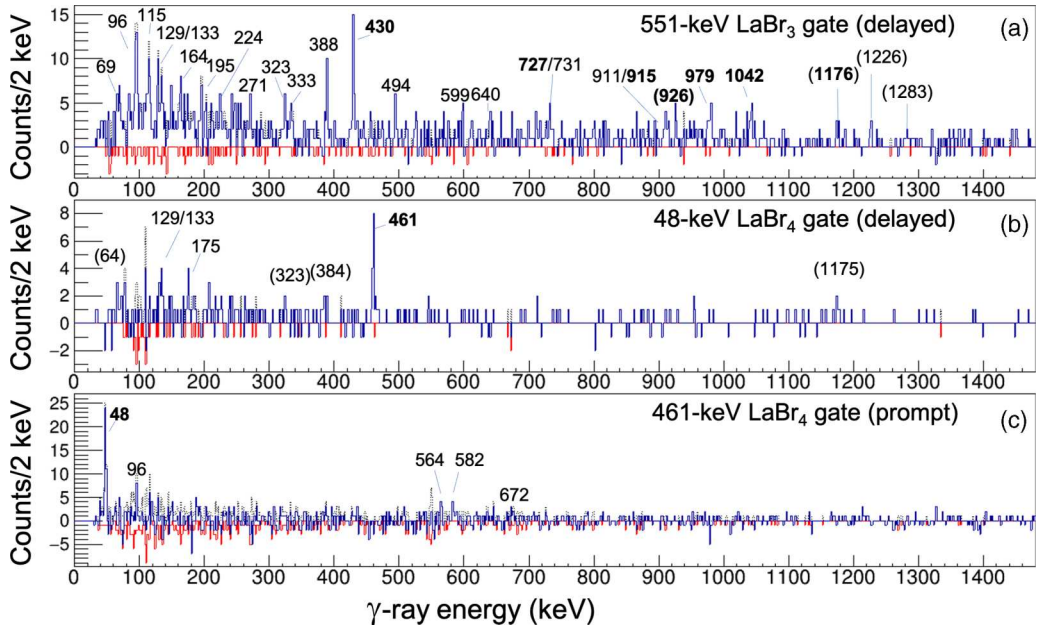

FIG. 6. Ge γ-ray spectra, obtained by gates on the $LaBr_3$ detectors. (a,b) Ge spectra obtained by delayed (2–70 ns) $LaBr_3$ gates on the 551-keV (a) and 48-keV (b) transitions. (c) Ge spectrum obtained by setting a prompt (−2 to 2 ns) $LaBr_3$ gate on the 461-keV transition. The background-subtracted spectra are shown in blue; the background spectra, in red, were plotted for comparison along the negative y axis, with the dotted lines showing the spectra prior to background subtraction. The energy labels are in keV, and those in bold correspond to γ rays placed in the level scheme in Fig. 8. See text for further details.

feed directly the 592-keV state. Other coincident γ rays are listed in Table I. Those included in the level scheme are shown in bold.

IV. DISCUSSION

The main results to be discussed are the low-lying isomeric states revealed by the detection of the 48-keV γ ray. In this section, from a comparison with systematics and theoretical predictions, possible spin and parity assignments for the 0.9(3) and 0.95(30) MeV states are considered.

The nonobservation of a γ ray emitted by the 0.9(3)-MeV state implies either a strongly converted decay, or a lifetime too long to be measured with the current setup. Specifically, for an isomeric transition of similar intensity as the 461- and 48-keV peaks, simulations reveal that for the exponential decay to be visible above the TDC background, its lifetime needs to be smaller than ≈200 ns, otherwise the counts would be scattered over a range too wide for a meaningful fit. A detailed examination of possible spin values reveals that the spin of the 0.9(3)-MeV state can at least in part be experimentally constrained. If one considers the lowest-spin collective states discussed in literature [54] and seen in neighboring nuclei, the most likely candidates are a one-phonon 1^- or 0^- octupole state, or a one-phonon 0^+ or 2^+ quadrupole state. In all of these cases, however, transitions to the ground-state and 2^- bands would be fast ($\lesssim$ ns), and would have been observed.

In neighboring even-even ^{250}Cf [28], for example, there are three low-lying collective states—a 2^+ γ vibrational state at 1031 keV, a 0^+ state at 1154 keV and a 1^- octupole vibrational state at 1175 keV—and they all decay via fast γ-ray decays to the ground-state band and/or the 2^- octupole band. The comparison with ^{250}Cf suggest that the 0.9(3)-MeV level in ^{248}Cf is unlikely to be a low-spin collective state.

In other neighboring isotopes, low-spin K isomers with an energy of approximately 1 MeV were found in ^{250}Fm (2^- at 881 keV [55]), ^{252}No (2^- at 929 keV [56]), and ^{254}No (3^+ at 988 keV [57]). These states also all decay via non-delayed γ-ray transitions to levels of the ground-state band. The 0.9(3)-MeV state in ^{248}Cf thus seems most likely to be a K isomer with a K large enough to make its decay too long to be detected by our setup (i.e., larger than approximately 200 ns).

The systematics of hindrance factor F_W vs ΔK from Ref. [52] permit one to deduce a likely lower limit for the K of the 0.9(3)-MeV state. For a $\Delta K = 2$, $F_W < 1 \times 10^6$ and $F_W < 1 \times 10^4$ can be expected for $E1$ and $M1$ transitions, respectively. These hindrances translate into lifetimes shorter than 15 ns for $E1$ and 20 ns for $M1$ transitions, assuming an energy of ≈250 keV for γ rays connecting a $K = J = 4$, 900-keV level to states of the $K = 2^-$ band. Such transitions would be fast enough to be observed in the current experiment. A lower ΔK would imply even shorter lifetimes. Only a $\Delta K \geqslant 3$ leads to delays in the range of hundreds of nanoseconds, or larger. Assuming a nearly 100% branching to the $K = 2$ band (since decays to the ground state band would be further hindered by the larger ΔK), the decay half-life of a $K = J = 5$ state at 900 keV to the lower lying $K = 2, 4^-$ level is estimated to be ≈750 ns for an $E1$ and ≈200 ns for an $M1$ transition ($F_W = 5 \times 10^7$ and 1×10^5, respectively). Hence, for the 0.9(3)-MeV state, a $K \geqslant 5$ seems most likely. Let us now consider a few plausible scenarios for the K assignment.

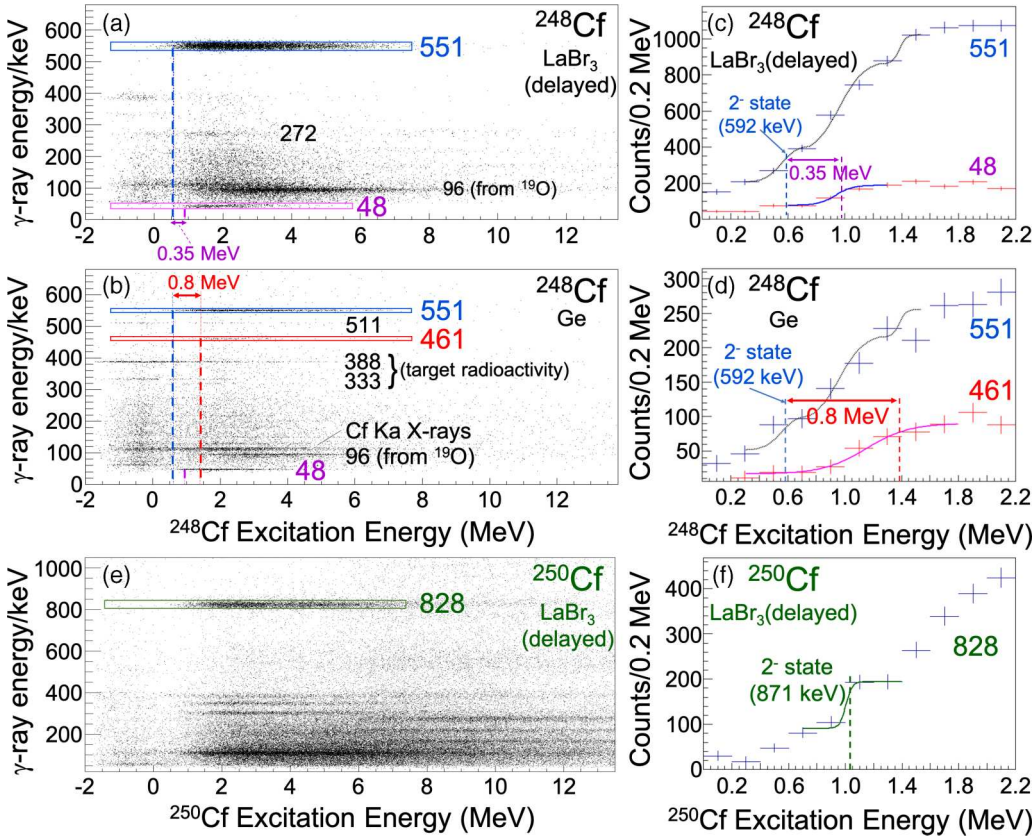

FIG. 7. γ-ray energy vs ^{248}Cf excitation-energy spectra for delayed $LaBr_3$ (a) and prompt Ge (b) events obtained by the ^{19}O gate. (c,d) Projections on the excitation-energy axis of the γ-ray gates shown in (a) and (b). The data are fitted using sigmoid functions. The 551-keV gated data are fitted using three sigmoid functions, and the curve shown in (c) was only scaled in (d) keeping all other parameters constant. Excitation-energy differences are measured using the sigmoid of the 551-keV γ ray in proximity of the 592 keV state and those of the 48- and 461-keV γ rays, at 80% of the amplitude of the local maximum. These spectra give a clear indication that the 461- and 48-keV γ rays are emitted by states lying respectively $\approx$0.8 and $\approx$0.35 MeV higher in excitation than the 592-keV level. (e,f) The same as (a) and (c), but for ^{250}Cf gated on the ^{17}O ejectile, with the sigmoid fit to the 828-keV γ ray. See text for further details.

A. $K = 8$ hypothesis

In the literature, theoretical predictions of high-K isomers in ^{248}Cf and in neighboring nuclei are rather limited. Among the most recent works, we mention the self-consistent Hartree-Fock Bogoliubov mean-field calculations by Delaroche *et al.* [58] and the Skyrme energy-density functional calculations by Minkov *et al.* [59]. Both methods predict the lowest two-quasiparticle state to be a two-quasineutron $K = 8^-$, respectively at 1.01 and 1.276 MeV. The calculations of the quasiparticle-plus-phonon model by Ivanova *et al.* [37] also predict the lowest two-quasiparticle state, at 0.8 MeV, to be a $K^\pi = 8^-$ state based on the coupling of the $\nu 7/2^+[624] \otimes \nu 9/2^-[734]$ neutron orbitals. In the ENSDF database [26], this 8^- isomer is identified with the 1261 keV state observed by Katori *et al.* [22]. We note that while for the other $N = 150$ isotones shown in Fig. 1 the lifetime of the 8^- state is known, it has not been measured for the 1261-keV state in ^{248}Cf. The current assignment is based on the systematics of the region and (d, t) cross sections measured in Ref. [22].

The fact that very different models all predict $K^\pi = 8^-$ for the lowest-lying high-K isomer suggest that this may be the configuration of the long-lived 0.9(3)-MeV state. The uncertainty in the excitation energy is too large to exclude that this is the same 1261-keV state observed in the (d, t) reaction. On the other hand, this would imply that the states emitting the 48- and 461-keV γ rays lie respectively at 1309 and 1770 keV. From inspection of the plots shown in Figs. 7(c) and 7(d), this seems unlikely, but possible.

In turn, for a $K^\pi = 8^-$ assignment of the 0.9(3) MeV state, the $E1$ multipolarity of the 48-keV transition restricts the spin-party of the 0.95(30) MeV state to 7^+, 8^+, or 9^+. No such states are predicted in Ref. [58], where the next two-quasineutron states are calculated, respectively, at 1.58 MeV $(7^-, 2^-)$, 1.81 MeV $(4^+, 3^+)$, and 1.99 MeV $(5^+, 2^+)$. The predicted lowest two-quasiproton states lie at 1.72 MeV $(2^+, 1^+)$, 1.78 MeV $(2^-, 5^-)$, 2.03 MeV $(6^+, 1^+)$, and 2.04 MeV $(3^-, 2^-)$. Possible candidates for the 0.95(30) MeV state may, however, be found in the calculations by Ivanova *et al.*, that include the two-quasineutron states $K^\pi = 7^+$ $(\nu 7/2^+[613] \otimes \nu 7/2^+[624])$ at 1.3 MeV and 8^+ $(\nu 9/2^-[734] \otimes \nu 7/2^-[743])$ at 1.5 MeV.

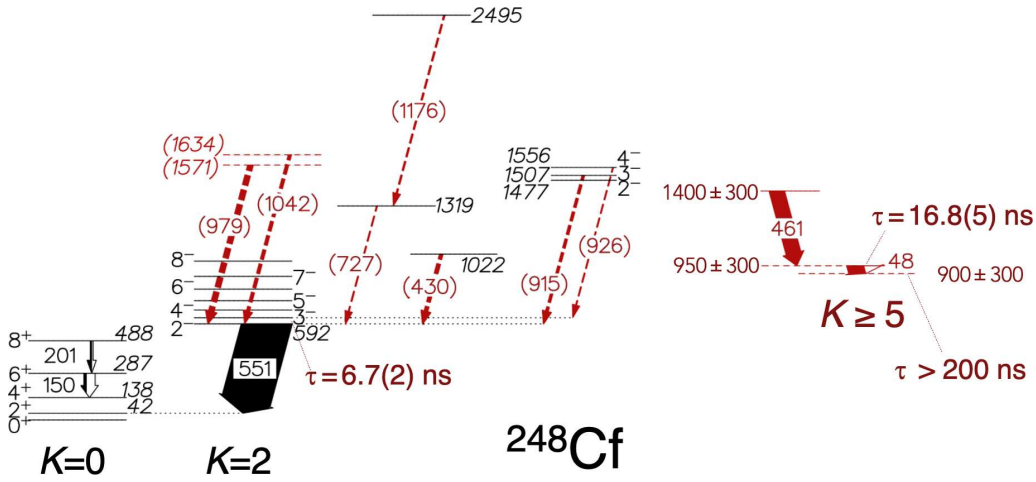

FIG. 8. Partial level scheme of ^{248}Cf, obtained combining the results of this experiment with information available in the literature [26]. New transitions observed in this work are shown in red, as well as the new proposed excited states. The width of the arrows is proportional to the observed γ-ray intensity; for established $E1$ and $E2$ transitions the converted fraction appears in white. Those γ rays whose placement is only tentative are represented by dashed arrows. For simplicity, the levels extending the ground-state and 2^- bands up to high spin from Ref. [27] were not included. For previously known levels, the energies determined in the (d,t) reaction [22] are used. Our γ-ray energies are in agreement with the published data within the uncertainty.

B. $K = 5$ hypothesis

An alternative configuration for the 0.9(3) MeV isomer seems also worthy of consideration. Calculations by the independent quasiparticle model predict a $K^\pi = 5^-$ state at 0.9 MeV [37], based on the proton $\pi 3/2^-[521] \otimes \pi 7/2^+[633]$ orbitals. In Ref. [58], this same state is predicted at a much higher energy, 1.78 MeV. One of the possible reasons for such difference is that in Ref. [37], the $3/2^-$ and $7/2^+$ proton orbitals are almost degenerate in energy. We notice that these orbitals, coupled to 2^- instead of 5^-, have been identified as a major component of the collective 2^- bandhead at 592 keV; see Ref. [34]. In fact, it has been argued [30,34] that their degeneracy is responsible for the strong coupling that lowers the 2^- band in ^{248}Cf. This degeneracy is furthermore supported by the low-lying structure of the neighboring isotopes ^{247}Bk ($Z = 97$, $N = 150$), ^{249}Bk ($Z = 97$, $N = 152$), and ^{251}Es ($Z = 99$, $N = 152$), where the two lowest lying states, $7/2^+$ and $3/2^-$, are separated by a mere 40.8(1) [60], 8.78(1) [61], and 8.4(1.0) keV [62]. It is conceivable that self-consistent calculations that predict a gap between these two proton orbitals at $Z = 98$, would not calculate the 5^- state to lie at such a low energy.

For a $K^\pi = 5^-$ 0.9(3)-MeV state, the spin-parity of the 0.95(30)-MeV level can only be 4^+, 5^+, or 6^+. Reference [37] lists possible candidates, but at significantly higher energy: a 6^+ two-quasineutron state at 1.6 MeV and 5^+ and 4^+ two-quasiproton states respectively at 1.7 and 1.8 MeV. Similarly, Delaroche [58] predicts 4^+ and 5^+ two-quasineutron states at 1.81 and 1.99 MeV and a 6^+ two-quasiproton state at 2.03 MeV.

The only other actinide in the region where a $K^\pi = 5^-$ band has been observed is ^{250}Cf, with the 5^- bandhead at 1396 keV [28]. Yates *et al.* populated this band both via (d, p) and via (α, t) reactions [63], and deduced a mixed configuration based on the proton $\pi 3/2[521] \otimes \pi 7/2[633]$ and the neutron $\nu 9/2[734] \otimes \nu 1/2[620]$ orbitals. Notably, in ^{250}Cf the neutron-proton admixture also explains a strong γ-ray transition proceeding from this state to a lower-lying 4^- band, as well as feeding γ rays from the $K = 5^-$ two-quasineutron band above. Such proton/neutron mixture may characterize also the states decaying to the 0.9(3) MeV state. We note that for ^{250}Cf the calculations in Ref. [37] predict the lowest two-quasiproton and two-quasineutron 5^- states at, respectively, 1.0 and 1.4 MeV.

Here we limit the discussion to the two lowest-lying high-K configurations predicted by calculations. Eventually, the spin and parity of the 0.9(3) MeV state in ^{248}Cf can only be determined with confidence by measuring its lifetime. Furthermore, the detection of this isomer decay is paramount to ascertain its energy and understand whether this is a new state or the previously observed 1261-keV level.

V. CONCLUSION

New excited states in ^{248}Cf were identified via in-beam γ-ray spectroscopy at the JAEA Tandem accelerator. For some γ rays, decay lifetimes in the nanosecond range were measured for the first time, leading to the measurement of two $B(E1)$ values for key low-lying transitions. One is the 551-keV γ ray that links the 2^- octupole vibrational to the ground-state vibrational band, the other is a newly observed 48-keV transition connecting two states respectively at 0.95(30) and 0.9(3) MeV. The lower limit on the lifetime of the 0.9(3)-MeV state was estimated to be $\approx$200 ns. Comparison with theoretical calculations suggests that possible configurations for this long-lived isomer are the two-quasineutron $K^\pi = 8^-$ and the two-quasiproton $K^\pi = 5^-$. A dedicated experiment is required to verify its configuration. Such a measurement would permit to better understand the role played by proton and neutron orbits near the $Z = 100$ and $N = 152$ deformed shell gaps, and provide an important

benchmark for theoretical calculations of heavy and superheavy nuclei.

ACKNOWLEDGMENTS

The authors express their gratitude to the JAEA Tandem accelerator crew for providing a stable ^{18}O beam and for their continued support. This work was partly supported by the REIMEI research grant of Advanced Science Research Center, Japan Atomic Energy Agency. E.I. acknowledges the support by the International Joint Research Promotion Program of Osaka University, and Japan Society for the Promotion of Science (JSPS) KAKENHI Grant No. JP 17H02893. T.T.P. acknowledges support from Japan Atomic Energy Agency as a special research student. We thank Y. Utsuno and K. Yoshida for fruitful discussions.

[1] A. Sobiczewski, F. A. Gareev, and B. N. Kalinkin, Phys. Lett. **22**, 500 (1966).
[2] W. D. Myers and W. Świątecki, Nucl. Phys. **81**, 1 (1966).
[3] V. E. Viola Jr. and G. T. Seaborg, J. Inorg. Nucl. Chem. **28**, 741 (1966).
[4] S. G. Nilsson *et al.*, Nucl. Phys. A **115**, 545 (1968).
[5] S. G. Nilsson *et al.*, Nucl. Phys. A **131**, 1 (1969).
[6] Z. Patyk and A. Sobiczewski, Nucl. Phys. A **533**, 132 (1991).
[7] S. Ćwiok *et al.*, Nucl. Phys. A **611**, 211 (1996).
[8] K. Rutz, M. Bender, T. Bürvenich, T. Schilling, P.-G. Reinhard, J. A. Maruhn, and W. Greiner, Phys. Rev. C **56**, 238 (1997).
[9] M. Bender, K. Rutz, P.-G. Reinhard, J. A. Maruhn, and W. Greiner, Phys. Rev. C **60**, 034304 (1999).
[10] Y. T. Oganessian and V. K. Utyonkov, Rep. Prog. Phys. **78**, 036301 (2015).
[11] P. J. Karol, R. C. Barber, B. M. Sherrill, E. Vardaci, and T. Q. Yamazaki, Pure Appl. Chem. **88**, 139 (2016).
[12] B. Singh, Nucl. Data Sheets **156**, 70 (2019).
[13] Y. Oganessian, J. Phys. G: Nucl. Part. Phys. **34**, R165 (2007).
[14] R. R. Chasman, I. Ahmad, A. M. Friedman, and J. R. Erskine, Rev. Mod. Phys. **49**, 833 (1977).
[15] C. Theisen *et al.*, Nucl. Phys. A **944**, 333 (2015).
[16] A. Sobiczewski, I. Muntian, and Z. Patyk, Phys. Rev. C **63**, 034306 (2001).
[17] A. V. Afanasjev, T. L. Khoo, S. Frauendorf, G. A. Lalazissis, and I. Ahmad, Phys. Rev. C **67**, 024309 (2003).
[18] M. Bender *et al.*, Nucl. Phys. A **723**, 354 (2003).
[19] P. T. Greenlees, J. Rubert, J. Piot, B. J. P. Gall, L. L. Andersson, M. Asai *et al.*, Phys. Rev. Lett. **109**, 012501 (2012).
[20] M. Asai, K. Tsukada, Y. Kasamatsu, Y. Ishii, A. Toyoshima, T. K. Sato *et al.*, JAEA-Tokai Tandem Annual Report 2013, p. 9.
[21] S. W. Yates, R. R. Chasman, A. M. Friedman, I. Ahmad, and K. Katori, Phys. Rev. C **12**, 442 (1975).
[22] K. Katori, I. Ahmad, and A. M. Friedman, Phys. Rev. C **78**, 014301 (2008).
[23] H. C. Griffin, I. Ahmad, A. M. Friedman, and L. E. Glendenning, Nucl. Phys. A **303**, 265 (1978).
[24] I. Ahmad and J. L. Lerner, Nucl. Phys. A **413**, 423 (1984).
[25] R. Takahashi, T. Ishii, M. Asai, D. Nagae, H. Makii, K. Tsukada *et al.*, Phys. Rev. C **81**, 057303 (2010).
[26] M. J. Martin, Nucl. Data Sheets **122**, 377 (2014).
[27] S. S. Hota, Ph.D. thesis, University of Massachusetts–Lowell, 2012 (unpublished).
[28] Y. Akovali, Nucl. Data Sheets **94**, 131 (2001).
[29] A. M. Mattera, S. Zhu, A. B. Hayes, and E. A. Mccutchan, Nucl. Data Sheets **172**, 543 (2021).
[30] A. P. Robinson, T. L. Khoo, I. Ahmad, S. K. Tandel, F. G. Kondev, T. Nakatsukasa *et al.*, Phys. Rev. C **78**, 034308 (2008).
[31] R. V. Jolos, L. A. Malov, N. Y. Shirikova, and A. V. Sushkov, J. Phys. G: Nucl. Part. Phys. **38**, 115103 (2011).
[32] Y.-S. Chen, Y. Sun, and Z.-C. Gao, Phys. Rev. C **77**, 061305(R) (2008).
[33] J. Zhao, B.-N. Lu, E.-G. Zhao, and S.-G. Zhou, Phys. Rev. C **86**, 057304 (2012).
[34] K. Rezynkina, A. Lopez-Martens, K. Hauschild, I. Deloncle, S. Péru, P. Brionnet *et al.*, Phys. Rev. C **97**, 054332 (2018).
[35] K. Yoshida, Phys. Rev. C **104**, 024318 (2021).
[36] V. G. Soloviev and T. Siklos, Nucl. Phys. **59**, 145 (1964).
[37] S. P. Ivanova, A. L. Komov, L. A. Malov, and V. G. Solovev, Fiz. Elem. Chastits At.Yadra **7**, 450 (1976); Sov. J. Part. Nucl. **7**, 175 (1976).
[38] K. Abusaleem, Nucl. Data Sheets **112**, 2129 (2011).
[39] S. Tanaka, K. Hirose, K. Nishio, K. R. Kean, H. Makii, R. Orlandi, K. Tsukada, and Y. Aritomo, Phys. Rev. C **105**, L021602 (2022).
[40] M. J. Vermeulen, K. Nishio, K. Hirose, K. R. Kean, H. Makii, R. Orlandi *et al.*, Phys. Rev. C **102**, 054610 (2020).
[41] K. R. Kean, K. Nishio, K. Hirose, M. J. Vermeulen, H. Makii, R. Orlandi *et al.*, Phys. Rev. C **100**, 014611 (2019).
[42] M. Wang *et al.*, Chin. Phys. C **45**, 030003 (2021).
[43] R. Léguillon, K. Nishio, K. Hirose, H. Makii, I. Nishinaka *et al.*, Phys. Lett. B **761**, 125 (2016).
[44] K. Hirose, K. Nishio, S. Tanaka, R. Léguillon, H. Makii, I. Nishinaka *et al.*, Phys. Rev. Lett. **119**, 222501 (2017).
[45] S. Q. Yan *et al.*, Astrophys. J. **919**, 84 (2021).
[46] S. Q. Yan *et al.*, Astrophys. J. **848**, 98 (2017).
[47] S. Q. Yan, Z. H. Li, Y. B. Wang, K. Nishio, H. Makii, J. Su *et al.*, Phys. Rev. C **94**, 015804 (2016)
[48] H. Makii *et al.*, Nucl. Instrum. Methods Phys. Res. Sect. A **797**, 83 (2015).
[49] T. Kibédi *et al.*, Nucl. Instrum. Methods Phys. Res. Sect. A **589**, 202 (2008).
[50] I. Ahmad, A. M. Friedman, R. F. Barnes, R. K. Sjoblom, J. Milsted, and P. R. Fields, Phys. Rev. **164**, 1537 (1967).
[51] K. E. G. Löbner, Phys. Lett. B **26**, 369 (1968).
[52] F. G. Kondev, G. D. Dracoulis, and T. Kibédi, At. Data Nucl. Data Tables **103-104**, 50 (2015).
[53] E. Browne and J. K. Tuli, Nucl. Data Sheets **108**, 681 (2007).
[54] P. C. Sood, D. M. Headly, and R. K. Sheline, At. Data Nucl. Data Tables **51**, 273 (1992).
[55] P. T. Greenlees, R. D. Herzberg, S. Ketelhut, P. A. Butler, P. Chowdhury, T. Grahn *et al.*, Phys. Rev. C **78**, 021303(R) (2008).
[56] B. Sulignano *et al.*, Eur. Phys. J. A **33**, 327 (2007).

[57] S. K. Tandel, T. L. Khoo, D. Seweryniak, G. Mukherjee, I. Ahmad, B. Back *et al.*, Phys. Rev. Lett. **97**, 082502 (2006).
[58] J.-P. Delaroche, M. Girod, H. Goutte, and J. Libert, Nucl. Phys. A **771**, 103 (2006).
[59] N. Minkov, L. Bonneau, P. Quentin, J. Bartel, H. Molique, and D. Ivanova, Phys. Rev. C **105**, 044329 (2022).
[60] C. D. Nesaraja, Nucl. Data Sheets **125**, 395 (2015).
[61] I. Ahmad, F. G. Kondev, E. F. Moore, M. P. Carpenter, R. R. Chasman, J. P. Greene *et al.*, Phys. Rev. C **71**, 054305 (2005).
[62] F. P. Heßberger *et al.*, Eur. Phys. J. A **26**, 233 (2005).
[63] S. W. Yates, I. Ahmad, A. M. Friedman, K. Katori, C. Castaneda, and T. E. Ward, Phys. Rev. Lett. **36**, 1125 (1976).